Molecular Structure of the AlO_2 Dimer, Al_2O_4

Edet F. Archibong and Alain St-Amant*

Department of Chemistry, University of Ottawa, 10 Marie Curie, Ottawa, Ontario K1N 6N5, Canada

Received: April 23, 1998; In Final Form: June 10, 1998

We report the results of our investigation of some stationary points on the singlet and triplet potential energy surfaces of Al_2O_4, one of the products tentatively identified in the Al + O_2 reaction in cryogenic matrices. The computations are done at the SCF, MP2, B3LYP, and CCSD(T) levels using one-particle basis sets ranging from 6-311G(2d) to 6-311+G(3df). Several geometries are considered, and a structure with D_{2h} symmetry is found to be the most stable isomer. Electron correlation is important for the quantitative determination of the relative energies of the various isomers. Vibrational frequencies and isotopic frequency ratios are computed for the most stable structure, and a comparison is made with values determined from cryogenic matrix studies. The dissociation energy, D_e, for the process $Al_2O_4 \rightarrow 2AlO_2$ is estimated to be 183 kcal/mol.

Introduction

There is conclusive evidence that cyclic AlO_2 is a major product of the reactions of thermal or pulsed-laser evaporated Al atoms with O_2 in inert gas matrices.[1−4] The earliest tangible identification of cyclic AlO_2 in cryogenic matrices was made by Serebrennikov et al.[1] In their report, the weak band at 1096 cm^{-1} observed in the infrared (IR) spectra of Al + O_2 reaction products and the strong band at 496 cm^{-1} were assigned to the $\nu_1(a_1)$ O−O stretch and $\nu_2(a_1)$ Al−O symmetric stretch, respectively, of cyclic AlO_2 ($^2A_2$). From the $\nu_1(a_1)$ and $\nu_2(a_1)$ and the observed isotopic shifts, an estimate of the $\nu_3(b_2)$ fundamental was also provided.[1] Subsequently, Andrews and co-workers[4] performed a comprehensive study of the reactions of pulsed-laser evaporated Al atoms with O_2 and confirmed that the 496 cm^{-1} band indeed belonged to cyclic AlO_2. These authors also shed new light on some of the earlier controversial assignments pertaining to the Al + O_2 reaction products in inert matrices.[4]

In addition to experimental work, several computational studies have also been devoted to the determination of the structure, vibrational frequencies, and dissociation energies of cyclic AlO_2.[5−8] A very recent theoretical study indicates that the latter has a $^2A_2$ ground state with a $^2A_1$ state lying about 7 kcal/mol above.[8] The dissociation energy of the $^2A_2$ ground state is estimated to be 65 kcal/mol at the CCSD(T)/6-311+G-(3df) level.[8] The bonding in cyclic AlO_2 has also been discussed.[5,8]

On the basis of the analyses of experimental IR data, it has been proposed that in addition to cyclic MO_2 (M = Al, Ga, In, Tl), aggregate species corresponding to the superoxide dimer, $(MO_2)_2$, are produced in inert matrices. For example, Carlson and co-workers specifically identified the dimer of MO_2 (M = Ga, In, Tl) and proposed an O_2M-MO_2 structure of D_{2d} symmetry for these species.[9,10] More recent work has also indicated that the 490 and 511 cm^{-1} bands,[4] as well as a 590 cm^{-1} band,[11] in the infrared spectra of the Al + O_2 reaction products in solid argon could be due to a simple dimer of cyclic AlO_2. The assignments of the molecular structures and the IR bands of the $(MO_2)_2$ (M = Al, Ga, In, Tl) species from experimental data are rather tentative,[4,9,10] and complementary structural information from quantum chemical calculations is necessary for conclusive determination of the equilibrium structures of the dimers.

An important step toward understanding the structures and bonding in these dimers was taken by Nemukhin and Weinhold,[12] who reported preliminary investigation of some stationary points on the singlet potential energy surface of Al_2O_4 as part of their study of the dinuclear aluminum oxides with formula Al_2O_n ($n = 1-4$). In that study,[12] Al_2O_4 was described as a complex consisting of two twisted AlO_2 groups, with a distorted tetrahedral arrangement of oxygen atoms around one of the aluminum atoms. Subsequently, Nemukhin[11] expanded upon these earlier calculations[12] and suggested that an intense IR band at 590 cm^{-1} observed in the spectrum of the Al + O_2 matrix reaction products could be attributed to the AlO_2 dimer, Al_2O_4. The dissociation energy of $(AlO_2)_2$ was also estimated as 128 kcal/mol at the MP2 level.[11]

Very recently, using large one-particle basis sets, we reported[8] CCSD(T) and density functional theory (DFT) studies of the structures, harmonic vibrational frequencies, and dissociation energies of cyclic MO_2 (M = Al, Ga). One of the conclusions made in that study is that gradient-corrected DFT methods, in conjunction with large flexible one-particle basis sets, do not suffer the symmetry breaking problems associated with these systems in previous theoretical investigations.[5−7] The present study employs DFT- and traditional Hartree−Fock (HF)-based methods to explore the singlet and triplet potential energy surfaces of Al_2O_4 in order to determine the likely gas-phase equilibrium geometry of the aggregate. In the sections below, it is established that the singlet-state structure previously suggested[11,12] for Al_2O_4 is less stable than its triplet-state counterpart. In fact, on the basis of the energies of the various isomeric forms considered and the comparison of computed vibrational frequencies with available experimental data, we propose an alternative structure for Al_2O_4.

Computational Methods

Geometry optimizations are carried out for the singlet and triplet molecular structures at the HF level (restricted formalism for singlet, unrestricted for triplet). Utilizing the HF geometries

S1089-5639(98)01966-5 CCC: $15.00
Published on Web 08/05/1998

and force constants, we reoptimize the geometries using second-order Møller−Plesset perturbation theory (MP2). Geometry optimizations are also carried out using the B3LYP functional. The latter uses Beckes's 3-parameter hybrid exchange-correlation functional[13] with the Perdew−Wang gradient-corrected correlation functional (PW91)[14] replaced with the Lee−Yang−Parr gradient-corrected correlation functional (denoted LYP).[15] The basis sets developed by Pople and co-workers[16] are employed. The smallest one-particle basis set used is 6-311G-(2d), and the largest is 6-311+G(3df).

The stationary points are characterized by frequency calculations. The harmonic vibrational frequencies of Al_2O_4 are computed by analytic second derivative methods at all levels of theory. We also calculate single-point energies for selected structures using the coupled-cluster approach including single + double excitations and a perturbational estimate of triple excitations [CCSD(T)]. The MP2 and B3LYP geometries are employed for the CCSD(T) calculations. In all the MP2 and CCSD(T) calculations, the 14 lowest molecular orbitals (MOs) of Al_2O_4 are frozen. All calculations are carried out with the GAUSSIAN 94 program suite.[17]

Results and Discussion

Prediction of the ground-state structure of Al_2O_4 via an exhaustive ab initio potential energy surface search is practically impossible. Therefore, the geometries initially considered for optimizations are those tentatively suggested for the MO_2 (M = Al, Ga, In, Tl) dimers from the analyses of IR spectra[4,9,10] and those recently proposed for the $(MO_2)_2$ species where M is a transition metal.[18−20] In the following sections, we present the results of geometry optimizations and the energies of selected isomeric forms of Al_2O_4 in both the singlet and triplet electronic states. The singlet molecular structures are indicated by "**s**" and the triplet structures by "**t**". Unless otherwise indicated, the calculations reported in the sections below employ the 6-311G(2d) basis set, and the relative energies do not include corrections for zero point energies.

The optimized geometric parameters computed for the singlet and triplet structures of Al_2O_4 at the MP2 level are presented in Figure 1, and the relative energies of the various isomeric forms at the HF, MP2, and B3LYP levels may be found in Table 1. For discussion purposes, we find it convenient to anchor the relative energies on structure **1**, since to date, **1s** (singlet **1**) is the only structure that has been proposed for Al_2O_4 in previous computational studies.[11,12]

The results listed in Table 1 show that triplet **1**, that is, **1t**, is 63 kcal/mol more stable than **1s** at the HF level. However, inclusion of electron correlation at the MP2 level significantly stabilizes **1s** by roughly 50%, and the **1s**−**1t** energy gap is lowered to 31 kcal/mol. The B3LYP **1s**−**1t** energy gap is computed to be 34 kcal/mol. Spin contamination is not pronounced in the triplet calculations. $\langle S^2 \rangle$ is 2.034 at the UHF level and 2.007 at the B3LYP level. Both **1s** and **1t** are found to be local minima at all levels. Structures **2s** and **2t** are related to **1s** and **1t**, respectively, via rotation of O_2 about the C_2 axis. Vibrational frequency analyses indicate that the optimized geometries of planar **2s** and **2t** possess Hessian indexes of 1 each, that is, **2s** and **2t** are transition structures. The **2s** structure lies 31 and 35 kcal/mol above **2t** at the MP2 and B3LYP levels, respectively. Following the imaginary a_2 mode of **2s** leads to **1s**, while that of **2t** leads to **1t**. Structure **2t** is 9 kcal/mol above **1t** at the B3LYP and MP2 levels, and **2s** is also 9 kcal/mol above **1s** (i.e., 40 kcal/mol above **1t**) at the MP2 level. One conclusion at this point is that **1t** is considerably more stable than **1s**. This is further confirmed by an MP2/6-311G(2df) calculation (not included in the table) which places the triplet below the singlet by 30.6 kcal/mol.

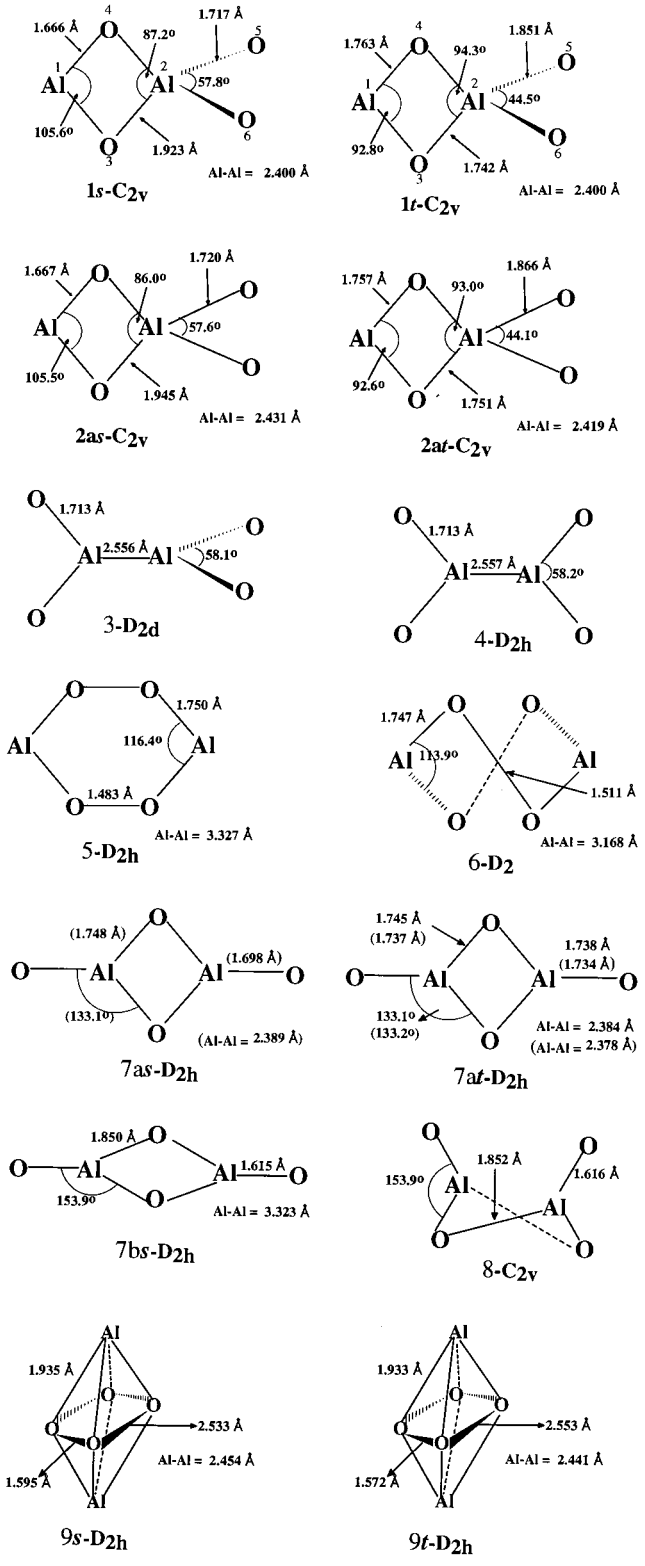

Figure 1. Structures of Al_2O_4 (**1**−**9**) investigated in this work. The optimized geometrical parameters are those obtained at the MP2/6-311G(2d) level. Those in brackets are B3LYP/6-311G(2d) geometrical parameters for **7as** and **7at**.

The geometries of the local minima **1s** and **1t** and the transition structures **2s** and **2t**, computed at the MP2 level, are included in Figure 1. First, we note that our calculated geometric parameters of **1s** are similar to the MP2/6-31G(d)

TABLE 1: Relative Energies[a,b] (kcal/mol) of Al_2O_4 Isomers Computed Using 6-311G(2d) Basis Set

	SCF	MP2	B3LYP
1s-C_{2v}	63.4	31.2	34.4
1t-C_{2v}	0.0	0.0	0.0
2s-C_{2v}	75.5	40.3	43.5
2t-C_{2v}	9.6	9.3	8.9
3s-D_{2d}	154.6	128.0	121.7
4s-D_{2h}	154.7	128.1	121.8
5s-D_{2h}	207.7	130.9	118.5
6s-D_2	178.0	119.2	115.9
7as-D_{2h}	139.0	*c*	36.2
7at-D_{2h}	5.7	−15.7	−22.2
7bs-D_{2h}	87.4	41.5	51.3
8s-C_{2v}		41.4	51.2
9s-D_{2h}	165.0	92.5	103.7
9t-D_{2h}	106.9	95.2	99.6

[a] Relative energies do not include corrections for zero point energies. [b] Total energies for the reference **1t** structure are given in Table 2. [c] Spurious solution obtained at the MP2 level. See text.

values reported by Nemukhin and Weinhold.[12] Noticeable differences can be observed between the geometries of **1s** and **1t** depicted in Figure 1. The bridge Al1−O3(O4) and the terminal Al2−O5(O6) distances are shorter by roughly 0.10 and 0.13 Å, respectively, in **1s**. Furthermore, the O3−O4 and O5−O6 distances and the O3−Al1−O4 and O6−Al2−O5 angles are reduced by 0.10 Å, 0.26 Å, 12.8°, and 13.3°, respectively, in **1t**. Natural population analysis indicates that natural charges on the terminal O5 and O6 are lowered by 0.84*e* on going from **1s** to **1t**. The Al−Al distance remains at 2.400 Å in both **1s** and **1t**. Note that the Al−Al distance in bulk Al is 2.86 Å. A qualitative explanation of the geometry change on going from **1s** to **1t** is provided by inspecting the highest occupied MO (HOMO) and the lowest unoccupied MO (LUMO) of **1s**. The triplet structure **1t** is derived by promoting an electron from the HOMO of **1s** to its LUMO. The HOMO is an antibonding a_2 symmetry orbital (π type) essentially localized on O5−O6, and the LUMO is a bonding a_1 symmetry orbital largely localized on O3−Al2−O4 with little contribution from Al1. Promoting an electron from the a_2 antibonding π orbital (HOMO in **1s**) located mainly on O5−O6 results in the shortening of this bond as observed in **1t**, and occupation of the a_1 bonding orbital (LUMO in **1s** but HOMO in **1t**) also results in a shortening of the O3−O4 distance.

Structures **3**-D_{2d} and **4**-D_{2h} may be viewed as simple dimers of AlO_2. The former structure is a minimum, and the latter is a transition structure for the relative rotation of the AlO_2 units about their principal axes. This rotation occurs virtually without a barrier (roughly 0.1 kcal/mol at all levels), in accord with the nearly identical geometric parameters computed for both structures (see Figure 1). Structural arrangements such as **3** and **4** have been suggested as possible candidates for MO_2 (M = Ga, In, Tl) dimers observed in matrix isolation studies. Our calculations, however, rule out **3** and **4** as viable contenders for the ground state of Al_2O_4. The results listed in Table 1 clearly show that both structures are over 120 kcal/mol above **1t**. Furthermore, the vibrational frequencies and the isotopic frequency shifts computed for the most intense bands of **3** do not fit the available experimental data. Since this study is essentially an attempt to elucidate and compute the vibrational frequencies and dissociation energy of the lowest-energy structure of the AlO_2 dimer (Al_2O_4), structures **3** and **4** and other high-energy structures depicted in Figure 1 will not be discussed further. The vibrational frequencies and the atomic coordinates of these species can be obtained from the authors.[21]

A possible structure for Al_2O_4 is **7**-D_{2h}. As depicted in Figure 1, this structure consists of an Al_2O_2 rhombic ring with terminal oxygen atoms on each aluminum atom. The structure may also be viewed as two AlO_2 units, with each unit consisting of nearly equivalent oxygen atoms. Two forms of **7** may also be distinguished. In **7a** the Al−Al distance is shorter than that in **7b**. The results in Table 1 suggest a **7as**−**7at** energy gap of 145 kcal/mol in favor of the triplet at the SCF level. However, on going from the SCF to the MP2 level, the singlet **7as** structure is unusually stabilized by as much as 322 kcal/mol (!) and the **7as**−**7at** energy gap is −177 kcal/mol at the MP2 level. The extent to which **7as** is stabilized by the inclusion of correlation effects at the MP2 level, in our experience, appears to be highly exaggerated and questionable. In marked contrast, B3LYP calculations place **7at** below **7as** by at least 58 kcal/mol. Again, the spin contamination is slight in the B3LYP triplet calculation with an $\langle S^2 \rangle$ value of 2.004 for **7at**.

To determine the reliability of the single-reference correlation treatment for **7as** and **7at**, we computed the $\mathcal{T}_1$ diagnostic at the CCSD level using the MP2 and B3LYP geometries. According to Lee et al.,[22−24] a $\mathcal{T}_1$ diagnostic value of 0.02 or greater indicates a significant multireference character large enough to cast serious doubt on the reliability of a single-reference correlation treatment. From our CCSD calculations using MP2 and B3LYP geometries, the $\mathcal{T}_1$ diagnostic value for **7as** is larger than 0.0375 and that of **7at** is less than 0.0140. It is obvious from these results that the correlated wave functions for **7as** exhibit significant multireference character, and this most likely explains the questionable stability of **7as** at the MP2 level. MP2 is not known as a method of choice when systems with large nondynamical electron correlation are considered. On the other hand, DFT includes the effect of electron correlation directly into an effective potential, and its efficacy for investigating difficult systems has been demonstrated.[25−27] Consequently, we consider the 58 kcal/mol predicted at the B3LYP level to be a reliable estimate of the **7as**−**7at** energy gap. While our resources do not permit elaborate multiconfigurational studies for a system of this size, our CCSD(T)//B3LYP calculations (though suspect for **7as**) suggest the **7as**−**7at** energy gap to be 39 kcal/mol, in qualitative agreement with the B3LYP result.

The results in Table 1 also indicate that, relative to **1t**, **7at** is 6 kcal/mol less stable at the Hartree−Fock level. Inclusion of electron correlation reverses the relative stability, and **7at** is more stable than **1t** by 16 and 22 kcal/mol at the MP2 and B3LYP levels, respectively. On the other hand, **7bs** is 42 kcal/mol higher in energy than **1t** at the B3LYP level and 51 kcal/mol higher at the MP2 level. Vibrational frequency analysis indicates that **7at** is a minimum whereas **7bs** has one imaginary frequency (11*i* cm^{-1}at MP2 and 19*i* cm^{-1} at B3LYP). Out-of-plane distortion of **7bs** does not result in any significant lowering of the energy of the resulting C_{2v} structure, **8**.

The energy separation between **1t** and **7at** is investigated further at the HF, MP2, and B3LYP levels using 6-311G(2df), 6-311+G(2df), and 6-311+G(3df) basis sets. The results listed in Table 2 confirm the reversal in the relative stabilities of **1t** and **7at** with the inclusion of electron correlation. Enlarging the one-particle basis sets from 6-311G(2d) to 6-311+G(3df) changes the relative energy by roughly 2.6, 0.4, and 1.0 kcal/mol at the HF, MP2, and B3LYP levels, respectively. Correcting for zero point vibrational energy affects the energy differences by less than 0.6 kcal/mol. It is perhaps worth noting that while the B3LYP relative energies differ from their MP2 counterparts by 6.5 to 8.0 kcal/mol, the relative energies

TABLE 2: Total Energies (au) and Relative Energies[a] (kcal/mol) for 1t and 7at

	total energies		relative energies	
methods	**1t**	**7at**	**1t**	**7at**
HF/6-311G(2d)	−783.473 027	−783.463 933	0.0	5.7
HF/6-311G(2df)	−783.484 765	−783.479 231	0.0	3.5
HF/6-311+G(2df)	−783.489 438	−783.484 519	0.0	3.1
MP2/6-311G(2d)	−784.420 284	−784.445 252	0.0	−15.7
MP2/6-311G(2df)	−784.516 938	−784.539 969	0.0	−14.4
MP2/6-311+G(2df)	−784.527 506	−784.551 728	0.0	−15.2
MP2/6-311+G(3df)	−784.542 832	−784.567 209	0.0	−15.3
B3LYP/6-311G(2d)	−785.969 399	−786.004 817	0.0	−22.2
B3LYP/6-311G(2df)	−785.978 354	−786.013 776	0.0	−22.2
B3LYP/6-311+G(2df)	−785.984 952	−786.021 646	0.0	−23.0
B3LYP/6-311+G(3df)	−785.991 149	−786.028 094	0.0	−23.2
CCSD(T)/ 6-311G(2d)[b]	−784.451 911	−784.489 984	0.0	−23.9
CCSD(T)/ 6-311G(2d)[c]	−784.451 785	−784.489 978	0.0	−24.0

[a] The relative energies do not include corrections for zero point energies. [b] Computed at MP2/6-311G(2d) geometries. [c] Computed at B3LYP/6-311G(2d) geometries.

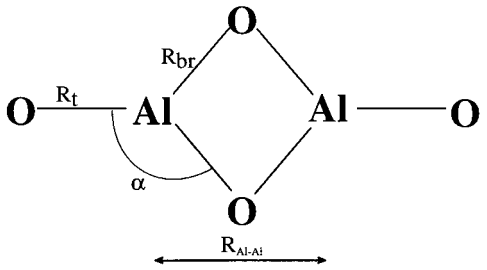

7a*t*-D$_{2h}$

Method	R_{Al-Al}/(Å)	R_{br}/(Å)	R_t/(Å)	α/(°)
HF/6-311G(*2d*)	2.367	1.707	1.655	133.8
HF/6-311G(*2df*)	2.361	1.706	1.653	133.8
HF/6-311+G(*2df*)	2.366	1.707	1.655	133.8
MP2/6-311G(*2d*)	2.384	1.745	1.738	133.1
MP2/6-311G(*2df*)	2.379	1.744	1.734	133.0
MP2/6-311+G(*2df*)	2.389	1.747	1.737	133.1
MP2/6-311+G(*3df*)	2.389	1.747	1.738	133.1
B3LYP/6-311G(*2d*)	2.378	1.737	1.734	133.2
B3LYP/6-311G(*2df*)	2.374	1.736	1.733	133.1
B3LYP/6-311+G(*2df*)	2.381	1.738	1.736	133.2
B3LYP/6-311+G(*3df*)	2.378	1.737	1.735	133.2

Figure 2. Optimized geometry of **7at** (the lowest-energy structure) at different levels of theory.

computed at the CCSD(T)/6-311G(2d) level using B3LYP/6-311G(2d) and MP2/6-311G(2d) geometries do not differ by more than 0.1 kcal/mol. On the basis of the CCSD(T) results, we predict **7at** to be more stable than **1t** by 24 kcal/mol. The very good agreement between the B3LYP and CCSD(T) predictions of the relative stability should also be noted. The results in Tables 1 and 2 suggest **7at** to be the most stable of the structures considered for Al_2O_4.

Results of geometry optimizations for **7at**-D_{2h} at different levels of theory are presented in Figure 2. First, the changes in the geometric parameters with basis sets are discussed. At the SCF level, the Al−Al distance computed with basis sets ranging from 6-311G(2d) to 6-311+G(3df) do not differ by more than 0.006 Å. The terminal and bridge Al−O distances are even more invariant on going from the smallest to the largest basis set. The bridge Al−O bond distance (R_{br}) differs by only 0.001 Å, and the terminal Al−O bond length (R_t) differs by 0.003 Å. At the MP2 and B3LYP levels, the changes in the bond distances with respect to enlargement of the basis sets from 6-311G(2d) to 6-311+G(3df) do not exceed 0.01 Å. In addition, the changes in the bond angle with respect to different basis sets do not exceed 0.1° at each level of theory. Next, the results in Figure 2 show the expected bond lengthening effect of electron correlation when flexible one-particle basis sets are used for geometry optimizations. The Al−Al distance changes the least with the inclusion of electron correlation. In all basis sets, the increase is roughly 0.02 Å at the MP2 level and between 0.011 and 0.015 Å at the B3LYP level. On the other hand, the terminal Al−O bond distance is most sensitive to electron correlation, increasing roughly by 0.08 Å at the MP2 and B3LYP levels. Electron correlation changes the O−Al−O angle by less than 1°.

Close inspection of the geometric parameters of **7at** reveals some finer trends. First, the bridge Al−O (R_{br}) and the terminal Al−O (R_t) bond distances do not differ by more than 0.01 Å at the MP2 level. In fact, B3LYP predicts R_{br} and R_t to be within 0.002 Å of each other using the 6-311+G(2df) and 6-311+G(3df) basis sets. It appears that R_{br} and R_t become closer with improved basis sets, and these bond distances might become even closer at higher levels of theory. It is important to note that inspection of the DFT orbitals does not indicate significant Al−Al interaction in **7at** despite the relatively short Al−Al distance. The ionic nature of **7at** is revealed by natural population analysis that places a total natural charge of +3.88 on the aluminum atoms.

The importance of computed harmonic vibrational frequencies as a complementary source of information for the correct interpretation of experimental infrared data cannot be overemphasized. Additionally, computed isotopic frequency shifts are nearly indispensable for proper identification of novel transient species formed in inert matrices. In Table 3, we list the computed harmonic vibrational frequencies and infrared intensi-

TABLE 3: Harmonic Vibrational Frequencies (cm^{-1}), Infrared Intensities (in Parentheses, km/mol) for 7at[a]

	SCF/6-311G(2d)			MP2/6-311G(2d)			B3LYP/6-311G(2d)			B3LYP/6-311G(*2df*)		
	$Al_2{}^{16}O_4$	$Al_2{}^{18}O_4$	*R*(16/18)	$Al_2{}^{16}O_4$	$Al_2{}^{18}O_4$	*R*(16/18)	$Al_2{}^{16}O_4$	$Al_2{}^{18}O_4$	*R*(16/18)	$Al_2{}^{16}O_4$	$Al_2{}^{18}O_4$	*R*(16/18)
a_g	1040	1017		967	947		959	939		962	942	
	825	779		733	692		737	696		736	694	
	450	433		415	399		410	394		408	393	
b_{2g}	242	239		210	207		210	207		207	205	
b_{3g}	740	712		679	654		677	653		679	654	
	278	269		218	211		213	206		210	203	
b_{1u}	981 (836)	956 (795)	1.0262	922 (449)	898 (429)	1.0267	915 (394)	891 (376)	1.0269	917 (391)	893 (373)	1.0266
	721 (9)	680 (7)		643 (46)	607 (40)		639 (49)	603 (43)		642 (48)	605 (42)	
b_{2u}	899 (350)	868 (332)	1.0357	810 (263)	782 (251)	1.0358	812 (257)	784 (245)	1.0357	811 (256)	783 (243)	1.0357
	196 (28)	187 (24)		155 (34)	147 (31)		148 (31)	141 (28)		147 (31)	140 (28)	
b_{3u}	452 (224)	438 (212)	1.0320	389 (154)	377 (147)	1.0318	388 (145)	376 (138)	1.0319	390 (145)	378 (138)	1.0317
	107 (11)	101 (9)		92 (12)	87 (11)		91 (11)	86 (10)		88 (11)	84 (10)	

[a] The isotopic frequency ratios *R*(16/18) are provided for the most intense bands.

ties of **7at**, the most stable structure of Al_2O_4 determined in this work. Also included are frequencies corresponding to the $Al_2{}^{18}O_4$ isotopomer and the $^{16}O/^{18}O$ isotopic ratio. Note that the molecule is in the *yz* plane and the harmonic vibrational frequencies reported in Table 3 are not scaled. The results in the table show that $\omega_7(b_{1u})$, $\omega_9(b_{2u})$, and $\omega_{11}(b_{3u})$ are the most intense vibrations. The $\omega_7(b_{1u})$ mode corresponds to antisymmetric ring motion, the $\omega_9(b_{2u})$ mode is the terminal Al−O antisymmetric stretch, and the $\omega_{11}(b_{3u})$ mode is an out-of-plane bending motion involving mainly the Al_2O_2 unit. As expected, the SCF harmonic frequencies are higher than their counterparts at the MP2 and B3LYP levels. The results also show that B3LYP harmonic frequencies are within 10 cm^{-1} of those computed at the MP2 level, and at the B3LYP level, increasing the size of the basis set from 6-311G(2d) to 6-311G(2df) changes the frequencies by less than 10 cm^{-1}. Using the B3LYP/6-311G(2df) results, intense bands are predicted for **7at** at 917 cm^{-1} (b_{1u}; 391 km/mol), 811 cm^{-1} (b_{2u}; 256 km/mol), and 390 cm^{-1} (b_{3u}; 145 km/mol). The $^{16}O/^{18}O$ isotopic ratio for these bands are 1.0266, 1.0357, and 1.0317, respectively.

Our computed vibrational frequencies may be compared with available experimental data from previous matrix isolation studies. It was mentioned in the Introduction that infrared spectra of M + O_2 (M = Al, Ga, In, Tl) reaction products in cryogenic matrices suggest the formation of M_2O_4.[4,9,10] In the case of Al_2O_4, it was reported[11] that a band at 590 cm^{-1} in the IR spectra of Al + O_2 reaction products might be evidence of the formation of **1s**. The B3LYP relative energies listed in Table 1 place **1s** roughly 34 kcal/mol above **1t** and 57 kcal/mol above **7at**. More important, the B3LYP/6-311G(2d) $^{16}O/^{18}O$ isotopic ratios of 1.0455 and 1.0488 that we computed for the intense bands of **1s** at 523 and 642 cm^{-1}, respectively, do not fit recent experimental data.[4] On the basis of these considerations, it is very doubtful that **1s** is the dimer of AlO_2 formed under conditions of stimulated aggregation in the matrix reaction.

Perhaps the most comprehensive work on the reaction of Al atoms with O_2 in inert matrices is that of Andrews and his associates.[4] These authors suggest in their report that the bands at 897.7, 843.2, and 808.1 cm^{-1} with $\nu(^{16}O)/\nu(^{18}O)$ ratios of 1.0264, 1.0306, and 1.0358 could be assigned to dimers containing two equivalent units of OAlO with each unit containing two equivalent oxygen atoms. Structures **1s** and **1t** do not fit the observed equivalence of two AlO_2 units. On the other hand, the strong bands at 917 and 811 cm^{-1} with $^{16}O/^{18}O$ isotopic ratios of 1.0266 and 1.0357 computed for **7at** agree quite well with the observed bands at 897.7 cm^{-1} and 808.1 cm^{-1} with isotopic ratios of 1.0264 and 1.0358, respectively. In addition, **7at** fulfils the criterion of having two equivalent AlO_2 units. The shortcoming of **7at**, however, is the slight inequivalence of the Al−O distances which differ by less than 0.005 Å in each AlO_2 unit (see B3LYP results in Figure 2). However the symmetry inequivalence of the oxygen atoms in each AlO_2 unit could be too small to resolve spectroscopically in matrix isolation studies. A similar situation was encountered and has been fully analyzed for the MO_4 alkali metal disuperoxides.[28,29] On the basis of these considerations, our results point to **7at** as the Al_2O_4 species observed in the reaction of Al + O_2 in inert matrices. The agreement between the computed and observed frequencies, in particular the computed and observed isotopic frequency shifts, strongly supports this assignment.

Finally, the dissociation energy, D_e, is estimated for the process $Al_2O_4(^3B_{1u}) \rightarrow 2AlO_2(^2A_2)$. The energies are computed at the B3LYP level since our prior studies on MO_2 (M = Al, Ga) indicate that DFT does not suffer from the symmetry breaking problems associated with cyclic AlO_2. The estimates are 180 kcal/mol, 181, 181, and 183 kcal/mol using 6-311G-(2d), 6-311G(2df), 6-311+G(2df), and 6-311+G(3df) basis sets, respectively. These results indicate that Al_2O_4 (**7at**) is quite stable toward dissociation affording two cyclic AlO_2 molecules.

Conclusion

The most stable gas-phase structure of Al_2O_4 on the singlet and triplet potential energy surfaces is found to be the D_{2h} structure depicted as **7at** in Figure 2. Vibrational frequencies and isotopic frequency ratios are computed and compared with values determined from matrix isolation studies. The agreement between the calculated and observed values is very good.

It is important to note that an exhaustive search of the potential energy hypersurface of Al_2O_4 has not been conducted. Doing so would lead to bankruptcy in terms of computer time. Instead, the structures have been carefully selected with particular attention paid to the structures tentatively suggested from experimental work. The most compelling corroborating evidence that the lowest-energy structure found in this study (**7at**) is indeed the one observed in matrix isolation studies is the excellent agreement between our computed vibrational frequencies (including the isotopic frequency shifts) and those reported from experimental IR studies. To suggest that **7at** is the global minimum on the potential energy hypersuface of Al_2O_4, without question, is probably unwise. Nevertheless, our results strongly suggest **7at** as being that isomer of Al_2O_4 observed in matrix isolation studies, with a dissociation energy $[Al_2O_4(^3B_{1u}) \rightarrow 2AlO_2(^2A_2)]$ estimated to be 183 kcal/mol at the B3LYP/6-311+G(3df) level.

Acknowledgment. We wish to thank the Natural Sciences and Engineering Research Council of Canada and the University of Ottawa for financial support. E.F.A. thanks the Mississippi Center for Supercomputing Research for a very generous allocation of computer time.

References and Notes

(1) Serebrennikov, L. V.; Osin, S. B.; Maltsev, A. A. *J. Mol. Struct.* **1982**, *81*, 25.
(2) Rozhanskii, I. L.; Chertikhin, L. V.; Serebrennikov, V. F.; Shevel'kov, V. F. *Russ. J. Phys. Chem. (Transl. of Zh. Fiz. Khim.)* **1988**, *62*, 1215.
(3) Rozhanskii, I. L.; Serebrennikov, L. V.; Shevel'kov, A. F. *Russ. J. Phys. Chem. (Transl. of Zh. Fiz. Khim.)* **1990**, *64*, 276.
(4) Andrews, L.; Burkholder, T. R.; Yustein, J. T. *J. Phys. Chem.* **1992**, *96*, 10182.
(5) Rubio, J.; Ricart, J. M.; Illas, F. *J. Comput. Chem.* **1988**, *9*, 836.
(6) Nemukhin, A. V.; Almlof, J. *THEOCHEM* **1992**, *253*, 101.
(7) Marshall, P.; O'Connor, P. B.; Chan, W.; Kristof, P. V.; Goddard, J. D. In *Gas-Phase Metal Reactions*; Fontijn, A., Ed.; North-Holland: Amsterdam, 1992.
(8) Archibong, E. F.; St-Amant, A. *Chem. Phys. Lett.* **1998**, *284*, 331.
(9) Zehe, M. J.; Lynch, D. A., Jr.; Kelsall, B. J.; Carlson, K. D. *J. Phys. Chem.* **1979**, *83*, 656.
(10) Kelsall, B. J.; Carlson, K. D. *J. Phys. Chem.* **1980**, *84*, 951.
(11) Nemukhin, A. V. *THEOCHEM* **1994**, *315*, 225 and references therein.
(12) Nemukhin, A. V.; Weinhold, F. *J. Chem. Phys.* **1992**, *97*, 3420.
(13) Becke, A. D. *J. Chem. Phys.* **1993**, *98*, 5648.
(14) Perdew, J. P.; Wang, Y. *Phys. Rev. B* **1992**, *45*, 13244.
(15) Lee, C.; Yang, W.; Parr, R. G. *Phys. Rev. B* **1988**, *37*, 785.
(16) Hehre, W. J.; Radom, L.; Schleyer, P.v. R.; Pople, J. A. *Ab Initio Molecular Orbital Theory*; Wiley: New York, 1986.
(17) Frish, M. J.; Trucks, G. W.; Schlegel, H. B.; Gill, P. M. W.; Johnson, B. G.; Robb, M. A.; Cheeseman, J. R.; Keith, T. A.; Peterson, G. A.; Montgomery, J. A.; Raghavachari, K.; Al-Laham, M. A.; Zakrzewski, V. G.; Ortiz, J. V.; Foresman, J. B.; Cioslowski, J.; Stefanov, B. B.; Nanayakkara, A.; Challacombe, M.; Peng, C. Y.; Ayala, P. Y.; Chen, W.; Wong, M. W.; Andres, J. L.; Replogle, E. S.; Gomperts, R.; Martin, R. L.;

Fox, D. J.; Binkley, J. S.; DeFrees, D. J.; Baker, J.; Stewart, J. P.; Head-Gordon, M.; Gonzalez, C.; Pople, J. A. *GAUSSIAN 94*; Gaussian, Inc.: Pittsburgh, PA, 1995.

(18) Chertihin, G. V.; Saffel, W.; Yustein, J. T.; Andrews, L.; Neurock, M.; Ricca, A.; Bauschlicher, W., Jr. *J. Phys. Chem.* **1996**, *100*, 5261.

(19) Andrews, L.; Chertihin, G. V. *J. Phys. Chem. A* **1997**, *101*, 8547.

(20) Chertihin, G. V.; Citra, A.; Andrews, L.; Bauschlicher, C. W., Jr. *J. Phys. Chem. A* **1997**, *101*, 8793.

(21) st-amant@theory.chem.uottawa.ca.

(22) Lee, T. J.; Rice, J. E.; Scuseria, G. E.; Schaefer, H. F. *Theor. Chim. Acta* **1989**, *74*, 81.

(23) Lee, T. J.; Taylor, P. R. *Int. J. Quantum Chem., Quantum Chem. Symp.* **1989**, *23*, 199.

(24) Lee, T. J.; Rendell, A. P.; Taylor, P. R. *J. Phys. Chem.* **1990**, *94*, 5463.

(25) Jones, R. O. *J. Chem. Phys.* **1985**, *82*, 325.

(26) Ziegler, T. *Chem. Rev.* **1991**, *91*, 651.

(27) Murray, C. W.; Handy, N. C.; Amos, R. D. *J. Chem. Phys.* **1993**, *98*, 7145.

(28) Jacox, M. E.; Milligan, D. E. *Chem. Phys. Lett.* **1972**, *14*, 518.

(29) Andrews, L.; Hwang, J. T.; Trindle, C. *J. Phys. Chem.* **1973**, *77*, 1065.